SHORT COMMUNICATION

H. Cölfen
T. Pauck

Determination of particle size distributions with angström resolution

Dr. H. Cölfen (✉) · T. Pauck
Max-Planck-Institut für Kolloid- und
Grenzflächenforschung
Kolloidchemie
Kantstraße 55
14513 Teltow, Germany

Abstract An analytical ultracentrifugation technique for the determination of particle-size distributions is used which applies an ultracentrifuge with a scanning absorption optical system. Radial scans during a sedimentation velocity experiment yield the particle-size distribution. If the particles consist of several defined monodisperse species, we show that for dense inorganic colloids the resolution of the particle-size distribution is in the angström range. This is demonstrated for a Pt colloid (0.4–2 nm) and unstabilized ZnO (4–9 nm) during particle growth.

Such highly resolved particle-size distributions show that the analytical ultracentrifuge is an excellent and rapid tool for the study of particle growth mechanisms as no other fractionating analytical technique with almost atomar resolution is known up to now. Some potential applications arising from the applied ultracentrifuge technique are suggested.

Key words Analytical ultracentrifugation – sedimentation velocity – particle size distribution – colloids – particle growth

Introduction

The determination of particle sizes and particle-size distributions using the analytical ultracentrifuge is as old as the ultracentrifuge itself [1–7]. Initially, the particle-size distribution was calculated from the radial concentration profiles of the sedimenting particles at a fixed time using a photographic absorption record [5], a photographic Schlieren pattern which shows the radial refractive index gradient in the ultracentrifuge cell [8] or radial intensity/absorption records aquired with a photomultiplier [9] or a photoelectric scanner [10]. As all these techniques require an expensive analytical ultracentrifuge, Scholtan and Lange [11] introduced a method based on a turbidity measurement in a modified preparative ultracentrifuge. In contrast to the former methods, the concentration profile was measured as a function of time at a fixed radius. In principle, this allows the advantageous application of acceleration profiles. As already introduced by Cantow [9], the Mie light scattering theory [12] was applied to determine the quantitative particle-size distribution. The technique of Scholtan and Lange was further improved so that nowadays seven samples with particle diameters between 10 and 3000 nm can be measured simultaneously. It has become an important technique for particle-size characterization in some industrial companies [13–18]. Compared with other methods for the determination of particle-size distributions, ultracentrifugation proved to be the most efficient and reliable method [19, 20].

Due to the fractionation of the particles in the ultracentrifugal field, the resolution of the determined particle-size distribution is high. If the colloids are dense as it is the case for inorganic particles, the range of accessible particle sizes (limited by the maximum rotor speed) can be extended down to 1 nm and even lower. Using a modern analytical

ultracentrifuge (Beckman Optima XL-A) with a sophisticated scanning absorption optics, a typical measurement of such a particle-size distribution takes only about 30–60 min. Hence, the ultracentrifuge can be used to monitor slow particle growth of colloids in its initial steps. In this study, we report that particle-size distributions can be obtained with a resolution in the angström regime.

Materials and methods

Two colloidal systems were investigated. The first was platinum synthesized by reduction of platinumtetrachloride in water with formic acid in the presence of the stabilizer alkaloid dihydrocinchinolin as described in [21]. The colloid was dispersed in a mixture of acetic acid and methanol (5:1 by volume) using ultrasonic for 5–10 min. The density of the solvent at 25 °C was determined as 1.0182 g/ml and its viscosity as 0.01167 P. The density of the stabilized platinum particles was found to be that of bulk platinum as the stabilizer molecules exchange so quickly in solution that they do not contribute to the density of the sedimenting particle. High-resolution transmission electron micrographs show that the colloids are spherical particles [22].

The second colloidal system was ZnO which was prepared according to [23] by mixing aliquotic volumes of isopropanolic solutions of $Zn(Ac)_2$ (1 mmol/l) and 20 mmol/l NaOH. After dilution with isopropanol by a factor of 5, the resulting mixture was heated to 65 °C under reflux and vigorous stirring for 2 h. The time when the heating is started defines the origin of the time window in which the propagation of the reaction is monitored. The rate of ZnO formation by dehydration of the initially formed $Zn(OH)_2$ was found to depend on the water content of the isopropanol used. The water content also seems to determine the product polydispersity of the ZnO colloid. Further investigations are needed to quantify this dependence, but are out of the scope of the present paper. Samples were drawn from the reaction mixture after 40 min and subjected to ultracentrifugation. The density of the sedimenting ZnO was taken from the literature for bulk ZnO to be 5.66 g/ml [24] as no stabilizer was applied. The shape of the particles was found to be triangular, rather than spherical as seen by transmission electron microscopy.

A Beckman Optima XL-A analytical ultracentrifuge (Beckman, Spinco division, Palo Alto, CA) with a scanning absorption optics (200–800 nm, accuracy ±2 nm) was used for all measurements. The ultracentrifuge software corrects the measured light intensity I by the initial intensity I_0 to give the absorbance $\log I_0/I$ in dependence of the radius. In contrast to other ultracentrifuge methods applied for the determination of particle size distributions [11, 13–18], continuous radial scans with a step size of 50 μm were performed at different scan intervals. The Pt-colloid was investigated at 60,000 rpm, 25 °C, 380 nm and with a scan interval of 2 min. For the ZnO colloid, 25,000 rpm, 25 °C and 280 nm were used with a scan interval of 3 min.

Results and discussion

The raw experimental data for both systems are presented in Fig. 1. It can be seen that in both cases the particles are fractionated with the proceeding of the experiment and several steps become obvious in the radial concentration profile. Each step corresponds to a separate species. The radial concentration profile can be transformed into a sedimentation coefficient distribution (Eq. (1)) and then into an absolute particle-size distribution using Eq. (2):

$$s_i = \frac{\ln(r_i/r_m)}{\omega^2 t}, \tag{1}$$

$$d_i = \sqrt{\frac{18\,\eta\,s_i}{\rho_2 - \rho_1}}, \tag{2}$$

where ω is the angular velocity, r the radial distance to the center of rotation with the indices i = particle i, m = meniscus, d_i the particle diameter of i, η the solvent viscosity, s_i the sedimentation coefficient of i and ρ the density with the indices 1 for solvent and 2 for the particle. The sedimentation coefficient distribution (Eq. (1)) is calculated for a constant velocity of the particles where the centrifugal force acting on the particles is balanced by the frictional and buoyant forces (see equal spacings between the individual scans for each particle in Fig. 1).

Equation (2) implies validity of Stokes law meaning that the particles must be spherical. This is usually fulfilled for lattices but not in every case for inorganic colloids. If the particles are not spherical, the determined diameter is only that of an equivalent sphere. Furthermore, the particle size distributions calculated from Eq. (2) do not take diffusion into account which can become significant, especially in case of very small particles like those investigated in this work. Diffusion effects can almost be suppressed, if a sufficiently high speed is selected so that the transport processes in the ultracentrifuge cell are clearly dominated by sedimentation.

From Fig. 1 it becomes clear that one must carefully choose the radial scan for the evaluation of the particle-size distribution. In the early stages of the experiment, the fractionation of the different species in the mixture is not yet achieved, whereas in the late stage, larger particles may already have reached the cell bottom and can hence not be
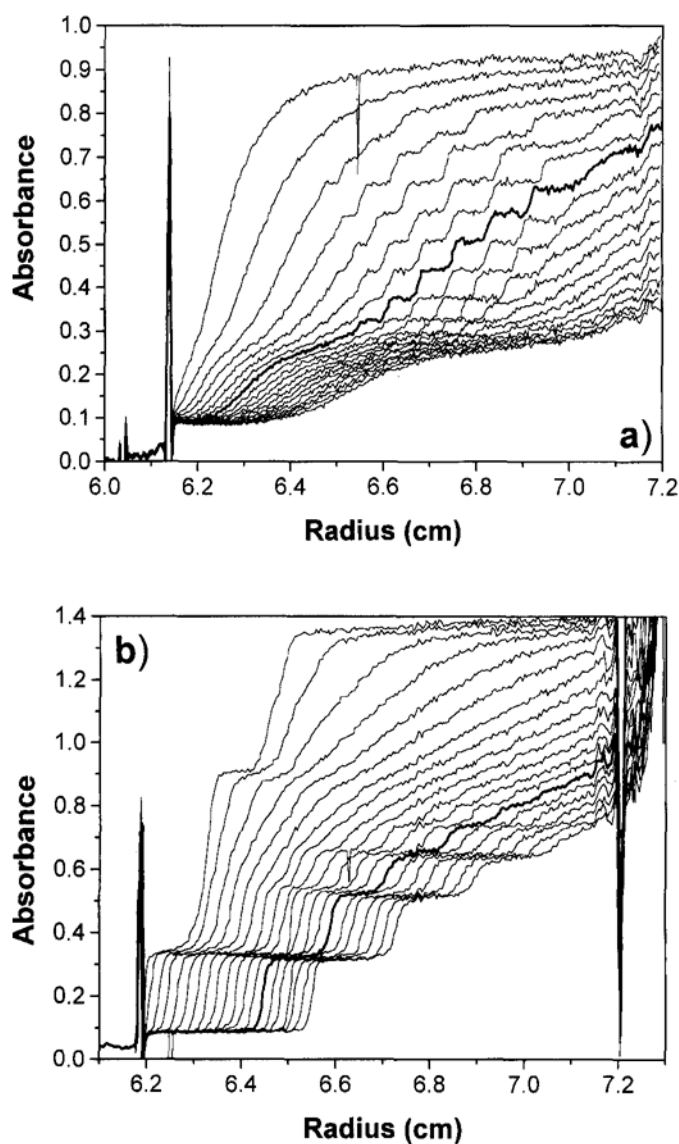
Fig. 1 Radial sedimentation velocity profiles at different times of centrifugation (absorbance $= \log I_0/I$ with I the light intensity): (a) Pt-colloid (Scan interval 2 min), (b) ZnO colloid (Scan interval 3 min). Both graphs are overlay plots of 20 individual radial scans

detected. Furthermore, wall effects with the cell bottom can then become significant. Therefore, only not too broad particle-size distributions can be investigated using radial scans at a constant rotational speed. If the dispersion should have such a broad particle-size distribution that it cannot be investigated at one speed, there is still the possibility to apply several speeds and to couple the derived particle-size distributions later on.

The application of several rotational speeds or of a speed profile was not necessary in case of the colloids investigated here. In both cases, radial scans could be found which represent all sedimenting species, e.g. the

complete particle-size distribution. These scans are marked as bold lines in Fig. 1. The corresponding particle-size distributions are presented in Fig. 2.

In both cases, a distinct number of monodisperse species is seen. The evaluation and comparison of the particle-size distribution for different radial scans for the same colloid taken at different centrifugation times yielded the same particle-size distribution for those particles which were already fractionated. This indicates that diffusion effects on the sedimentation coefficient distribution (leading to a sharpening of this distribution with time [25, 26] and hence to an apparent sharpening of the particle-size distribution with time [27]) are negligible. Also the self-sharpening of the boundary which can become pronounced especially for rod-like molecules [25] is negligible. Nevertheless, diffusion effects cannot be suppressed completely. This leads to slightly broadened peaks in the particle-size distribution like those shown in Fig. 2 although these peaks represent completely monodisperse species.

Due to the very small particle size, the relative absorbance of the individual species corresponds directly to their mass fraction if the extinction coefficient does not change with the particle size. This is assumed in this study. However, when using a combined absorption and refractive index detection as mounted on the new Beckman Optima XL-I, the extinction coefficient of each particle can be determined for transparent samples.

For the Pt-colloid, a continuous bimodal particle-size distribution is detected from electron microscopy with average particle sizes of 1.0 and 2.2 nm [22]. These two peaks can also be found with the same shape of the distribution in Fig. 1a but with a much better resolution for the bigger species. The particle sizes from the ultracentrifuge experiments are slightly smaller than those from electron microscopy. This can be attributed to the extremely small particles which are only clusters of few atoms. Here the particular character becomes important; thus the continuum approach of the Stokes–Einstein equation becomes a crude approximation. For larger particles, the particle size from ultracentrifuge measurements is usually found larger than that from electron microscopy. The reason is that the ultracentrifuge measures the size of the sedimenting particle (with stabilizer or hydrate shell).

The striking feature in Fig. 2a is the presence of resolved monodisperse species which only partly differ 1 Å in the particle diameter. The diameter of a platinum atom is 2.74 Å. If we assume that the platinum colloid already exhibits the cubic most dense spherical packing without distortions, the volume occupation is 74%. A volume calculation for the spherical platinum particles allows the determination of the number of atoms in each of the resolved species. The lower end of the particle-size distribution in Fig. 2a is about 4–5 Å which would correspond

Fig. 2 Integral and differential particle-size distributions of (a) Pt-colloid and (b) ZnO colloid
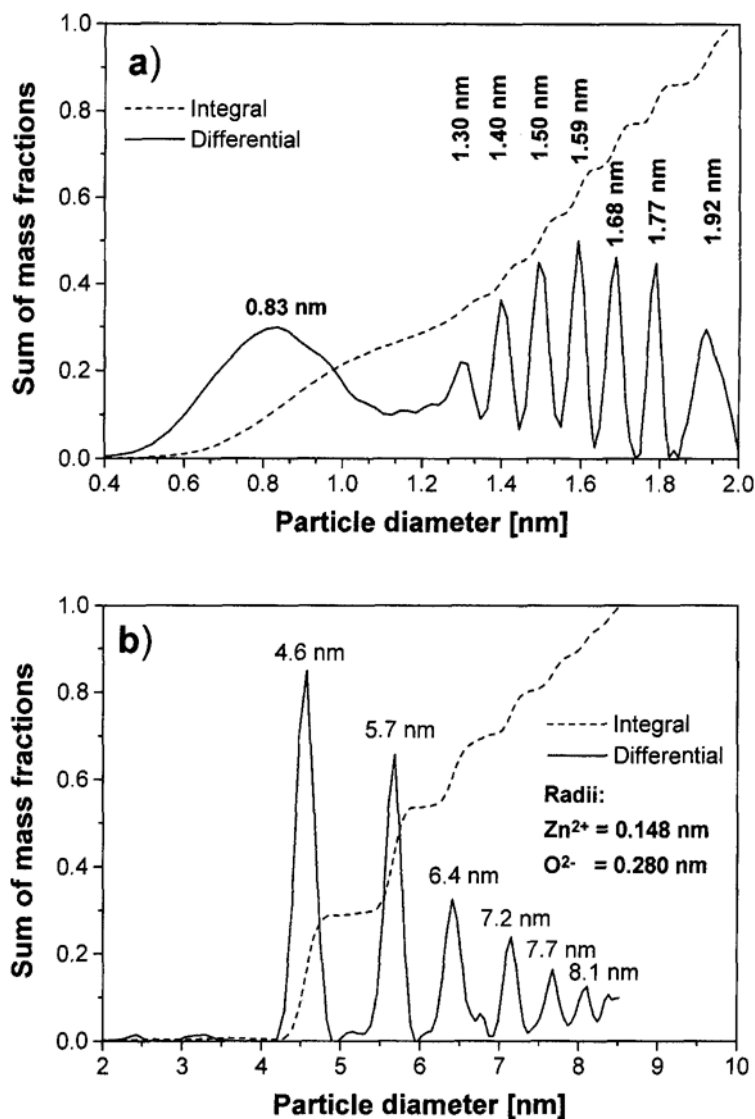
to just 2–4 platinum atoms. The maximum of the first peak at 8.3 Å (mass fraction 28%) corresponds to 21 atoms on the average. As such clusters are very small, the broad peak must be considered with some caution because it does not reflect the true particle-size distribution due to the expected high diffusivity for such small clusters. However, the particle-size distribution from electron microscopy shows a similar broadening [22].

The particles grow in a very defined manner resulting in several monodisperse species (atom number/mass fraction): 13 Å (79 atoms/9%), 14 Å (99 atoms/8%), 15 Å (121 atoms/11%), 15.9 Å (145 atoms/11%), 16.8 Å (171 atoms/10%), 17.7 Å (200 atoms/9%) and 19.2 Å (255 atoms/14%). This shows that the mass fraction of the monodisperse species is almost constant with 10%. The relative widths of Gaussian fits of the individual peaks in Fig. 2a are from small to big particles 42.4%, 5.3%, 3.1%, 2.7%, 2.3%, 2.2%, 1.8% and 4.7%. All of these peaks

(except the first) are very narrow underlining the monodispersity of the colloids. The Pt-particles show no magic numbers in their particle growth, but grow via a complete plating of one crystal surface. To determine the measurement error, the particle diameter were independently calculated from the movement of the corresponding boundaries taking multiple radial scans into account. The relative errors in the particle diameters were beyond 2% in most cases.

In case of the ZnO colloid, 6 monodisperse species are resolved (particle diameter/mass fraction): 46 Å/29%; 57 Å/25%; 64 Å/16%; 72 Å/11%; 77 Å/7%, 81 Å/7%; the remaining 5% are not resolved as separate species. This verifies a well-defined crystal growth for ZnO as well. In contrast to the monodisperse Pt-colloid species, the difference in the particle diameter of the resolved species as well as their mass fraction is not constant but overall decreasing with increasing particle size. This may be an effect of

the different crystallization speed at the different crystal faces of the ZnO (Wurtzit structure). A calculation of the number of ions from the particle size is not meaningful for ZnO because the particles are not spherical. Therefore, the determined particle-size distribution is only apparent. The relative error of the determined particle size is below 2% in all cases. The relative widths of the Gaussian fits in Fig. 2b are from small to big particles: 5.2%, 3.5%, 3.1%, 2.4%, 1.9% and 1.8%. This is an effect of the decreasing diffusion broadening with increasing particle size (relative width: 5.2% →1.8%). The same is found for the monodisperse Pt-species in Fig. 2a (relative width: 5.3% →1.8%).

Obviously, the applied ultracentrifugation studies allow a detailed study of particle growth mechanisms. Nevertheless, it must be pointed out that the particle size distribution is only apparent, if the shape of the particles is not spherical like it is the case for the ZnO colloid or if the density of the sedimenting particles is not known. The latter complication can be circumvented in an elegant way by the measurement of the same sample in two solvents of different density where a constant particle-size distribution can be assumed (e.g. H_2O, D_2O) [13,18].

Conclusions and outlook

We have shown that the ultracentrifuge is able to resolve particle-size distributions of particles with almost atomar resolution if the particles are small and have a high density. For this purpose, a commercially available analytical ultracentrifuge with a sophisticated UV-absorption optics (Beckman, Optima XL-A) is suitable without any modification. Nevertheless, still the restriction exists that the particle-size distribution must be narrow enough, so that one rotational speed is sufficient to fractionate all species.

This is the reason why usually the particle size is determined as a function of time at a constant location but with varying rotational speed [11,13–18]. However, this method applies a turbidity detector which cannot detect such small particles as investigated here. Especially if the dispersion has an intense color like it is the case for the Pt-colloid (black dispersion), any optical detection system of an analytical ultracentrifuge (turbidity, Schlieren or Rayleigh interference) except an absorption optics would

fail in the correct determination of the concentration profile as the light absorption is too intense, even in highly diluted systems.

In principle, it should also be possible to perform time-dependent sedimentation velocity profiles at a constant radius in the XL-A ultracentrifuge if the detector slit would be kept at a fixed radius [28]. This would have the big advantage that the detection wavelength could be chosen between 200 and 800 nm which is not possible with the turbidity detectors currently in use. The high sensitivity of absorption measurements would enable measurements at the lowest possible concentration if the absorption maximum is used as scanning wavelength. Furthermore, if complicated mixtures are to be investigated, there exists the potential chance that the individual particle-size distribution of each component can be determined if the particles absorb at sufficiently different wavelengths. However, the necessary application of rotor speed velocity profiles coupled with an on-line detection is not possible with the current ultracentrifuge software.

A further interesting feature of the performed determination of particle sizes using radial absorption scans is the possibility to measure absorption spectra at every desired radius in the ultracentrifuge cell. If now monodisperse species are detected in a radial scan like those in Fig. 1, the particle size and the current position of this species is known. At such radius, a spectrum can be recorded and be correlated to the particle size [29]. This is especially interesting for mesoscopic semiconductor materials where the band gap changes with the particle size due to spatial carrier confinement [30–32].

If a combined absorption/interference optics is used (the Beckman Optima XL-I ultracentrifuge for example), one can detect the concentration of each of the monodisperse particles in Fig. 1 via the recorded interference fringe shift, whereas the corresponding absorption is recorded with the absorption optics. The derived extinction coefficient can be correlated with the particle size and will be subject of a forthcoming paper.

References

1. Svedberg T, Rinde H (1924) J Am Chem Soc 46:2677
2. Rinde H (1928) The distribution of the sizes of particles of gold sols. PhD Thesis Upsala

3. Nichols JB (1931) Physics 1:254
4. Nichols JB, Kraemer EO, Bailey ED (1932) J Phys Chem 36:326

5. Nichols JB, Bailey ED, Kraemer EO (1932) Ultracentrifugal determination of the particle size of polychloropropene emulsions. 84th Meeting of the Am Chem Soc, Division of Colloid Chemistry, Denver

6. Bailey ED, Nichols JB, Kraemer EO (1934) Variation of light absorption with particle size of suspended material. 88th meeting of the Am Chem Soc, Division of Colloid Chemistry, Cleveland
7. Svedberg T, Pedersen KO (1940) Die Ultrazentrifuge. Steinkopff Verlag, Dresden, Leipzig, p 296
8. McCormick HW (1964) J Colloid Sci 19: 173
9. Cantow HJ (1964) Makromol Chem 70: 130
10. Aeijelts Averink JW, Reerink H, Boerma J, Jaspers WJM (1966) J Colloid Interface Sci 21:66
11. Scholtan W, Lange H (1972) Kolloid-Z, Z Polymere 250:782
12. Mie G (1908) Ann Physik 25:377
13. Mächtle W (1984) Makromol Chem 185:1025
14. Mächtle W (1988) Angew Makromol Chem 162:35

15. Müller HG (1989) Colloid Polym Sci 267:1113
16. Mächtle W (1992) Makromol Chem Macromol Symp 61:131
17. Mächtle W (1992) Analysis of polymer dispersions with an eight cell-AUC multiplexer: High resolution particle size distribution and density gradient techniques. In: Harding SE, Rowe AJ, Horton JC (eds) Analytical Ultracentrifugation in Biochemistry and Polymer Science, Ch 10. The Royal Society of Chemistry, Cambridge, p 147
18. Müller HG, Herrmann F (1995) Prog Colloid Polym Sci 99:114
19. Li J, Caldwell K, Mächtle W (1990) J Chromatography 517:361
20. Lange H (1995) Part Part Syst Charact 12:148
21. Bönnemann H, Braun GA (1996) Enantioselektive Hydrierung an Platinkolloiden; Angew Chem Int Ed 35:1992

22. Braun GA (1996) PhD Thesis, Mülheim, in preparation
23. Bahnemann DW, Kormann C, Hoffmann MR (1987) J Phys Chem 91:3789
24. CRC Handbook of Chemistry and Physics, 73rd ed (1992). CRC Press, Boca Raton, FL
25. Schachman HK (1959) Ultracentrifugation in Biochemistry. Academic Press, New York, London, p 137
26. Fujita H (1973) Foundations of Ultracentrifugal Analysis. Wiley, New York, p 176
27. Rapoport D, Vogel W, Cölfen H, Schlögl R (1996) J Chem Phys, submitted
28. Cölfen H (1995) unpublished
29. Pauck T, Cölfen H, Antonietti M (1996) in preparation
30. Weller H (1993) Adv Mater 5:88
31. Weller H (1993) Angew Chem 105:43
32. Schmitt-Rink S, Henneberger K, Göbel EO (1993) Optical Properties of Semiconductor Nanostructures. Akademie Verlag, Berlin